Cytogenesis in the Adult Monkey Motor Cortex: Perivascular NG2 Cells Are the Major Adult Born Cell Type

Gregory B. Stanton,[1]* Shawn J. Kohler,[1] Jennifer Boklweski,[1] Judy L. Cameron,[2] and William T. Greenough[1,3,4]†

[1]Beckman Institute, University of Illinois, Urbana, IL, 61801
[2]Department of Psychiatry, University of Pittsburgh, Pittsburgh, PA 15213
[3]Department of Psychology, University of Illinois, Urbana, IL, 61801
[4]Neuroscience Program, University of Illinois, Urbana, IL, 61801

ABSTRACT

We used confocal microscopy and immunohistochemistry (IHC) to look for new cells in the motor cortex of adult macaque monkeys that might form the cellular bases of improved brain function from exercise. Twenty-four female *Macaca fascicularis* monkeys divided into groups by age (10–12 years, 15–17 years), postexercise survival periods, and controls, received 10 weekly injections of the thymidine analog, bromodeoxyuridine (BrdU) to mark new cells. Sixteen monkeys survived 15 weeks (5 weeks postexercise) and 8 monkeys survived 27 weeks (12 weeks postexercise) after initial BrdU injections. Additionally, five *Macaca mulatta* female monkeys (~5.5–7 years) received single injections of BrdU and survived 2 days, 2 weeks, and 6 weeks after BrdU injections. Neural and glial antibodies were used to identify new cell phenotypes and to look for changes in proportions of these cells with respect to time and experimental conditions. No $BrdU^+/DCx^+$ cells were found but about 7.5% of new cells were calretinin-positive (Cr^+). $BrdU^+/GABA^+$ (gamma-aminobutyric acid) cells were also found but no new Cr^+ or $GABA^+$ cells colabeled with a mature neuron marker, NeuN or chondroitin sulfate antibody, NG2. The proportion of new cells that were $NG2^+$ was about 85% for short and long survival monkeys of which two, newly described perivascular phenotypes (Pldv and Elu) and a small percentage of pericytes (2.5%) comprised 44% and 51% of the new $NG2^+$ cells, respectively. Proportions of $NG2^+$ phenotypes were affected by post-BrdU survival periods, monkey age, and possibly a postexercise sedentary period but no direct effect of exercise was found. J. Comp. Neurol. 523:849–868, 2015.

INDEXING TERMS: exercise; confocal microscopy; polydendrocytes; pericytes; PDGFrβ; BrdU; calretinin; Olig2

Exercise is known to increase blood flow to the brain (Herholz et al., 1987) and the release of several neurotrophic factors (Klintsova et al., 2004; Leak et al., 2012; Voss et al., 2013), but relatively few studies have examined the cellular basis for improvement of brain function by exercise. Increased neuronal proliferation in the hippocampus of adult mice (Holmes et al., 2004; Olah et al., 2009) was found, but exercise did not promote neurogenesis in the motor, visual, or cingulate cortices (Ehninger and Kempermann, 2003). However, exercise did have an effect on neocortical gliogenesis. In wheel-running mice, there was an increase in layer 1 microglia in the motor cortex (Ehninger and Kempermann, 2003) and a decrease of new cells that coexpressed the proteoglycan, NG2, and the astrocyte marker, s100β, in the visual cortex (Ehninger 2011). And in adult mice with access to running wheels, $NG2^+$ cell proliferation was

†Died December 18, 2013.

Grant sponsor: National Institutes of Health; Grant number: AG10154; Grant sponsor: Kiwanis Spastic Paralysis Research Foundation; Grant sponsor: Retirement Research Foundation.

*CORRESPONDENCE TO: Gregory B. Stanton, Neurotech Group, Beckman Institute, 405 North Mathews Ave., Urbana, IL 61801.
E-mail: gbstantn@illinois.edu

Received January 26, 2014; Revised October 8, 2014;
Accepted October 8, 2014.
DOI 10.1002/cne.23693
Published online October 10, 2014 in Wiley Online Library (wileyonlinelibrary.com)

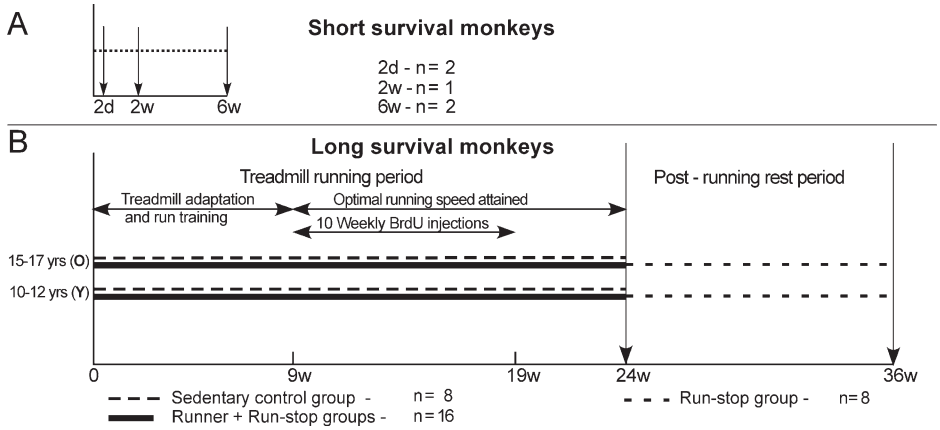

Figure 1. Timeline diagrams of monkey groups. **A:** Monkeys that received a single BrdU injection and survived short time intervals before perfusion (down arrows). **B:** Runner and sedentary control monkeys that received 10 weekly BrdU injections and survived 5 or 17 weeks after the injection period.

reduced but $NG2^+$ cell differentiation into mature oligodendrocytes was increased (Simon et al., 2011).

$NG2^+$ cells are the most abundant new cell type in the brains of adult rodents. Although early studies considered these cells to be multipotential neural and glial progenitor cells (Raff et al., 1983; Stallcup, 2002), the conclusion of recent cell fate studies in mice is that $NG2^+$ cells, in the form of polydendrocytes (Nishiyama et al., 2009), are almost exclusively oligodendrocyte precursor cells (Rivers et al., 2008; Dimou et al., 2008; Kang et al., 2010; Hughes et al., 2013). However, perivascular brain pericytes also express NG2 and, because they are angiogenic during brain development (Virgintino et al., 2007), injury (Diaz-Flores et al., 2009; Dore-Duffy and Cleary, 2011), or pathology (Helfer et al., 2009), it seems reasonable that they might be active during angiogenesis that results from exercise (Isaacs et al., 1992; Swain et al., 2003; Ding et al., 2006; Rhyu et al., 2010).

To date, there have been no studies of adult born $NG2^+$ cells in the monkey cerebral cortex. The current study examines new $NG2^+$ cells over several time intervals including two time periods following experimental exercise. In addition, we also examined the expression of other glial and neuronal markers of adult born cells. We focused on two goals: 1) categorizing the major phenotypes and relative proportions of adult born NG2 cells in the cerebral cortex, and 2) determining if any cell type is responsive to one or more variables of an experimental exercise protocol.

MATERIALS AND METHODS

Subjects

We used six adult female *Macaca mulatta* (ages ~5.5–7.0 years) and 24 adult female *Macaca fascicularis* (ages 10–17 years) for these experiments. The *M. fascicularis* monkeys were part of a larger study of the effects of exercise on the brain (Rhyu et al., 2010; Kohler et al., 2011). The monkeys were housed in pens approximately 2 m by 4.5 m by 3.3 m high within a social living group of 2–3 similar aged pen mates, or in individual cages. They were fed Purina Monkey Chow (no. 5045; Ralston-Purina, St. Louis, MO) once daily. Animals living in pens had both natural and artificial lighting, making the light/dark cycle equivalent to natural day length in the summer months and 0700 hours to 1900 hours in the winter months. Animals living in cages had lights on from 0700 hours to 1900 hours. All animal care and use and tissue procedures were conducted in accord with protocols approved by the Institutional Animal Care and Use Committees of the University of Pittsburgh and the University of Illinois and in accordance with NIH standards and guidelines.

Experimental design

The thymidine analog bromodeoxyuridine (BrdU) was administered by intraperitoneal injection in six *M. mulatta* monkeys as a single dose (100 mg/kg) under light sedation to study phenotype expression of BrdU-marked cells over short postinjection survivals (Fig. 1A). Two of these monkeys were sacrificed at 48 hours, two were sacrificed at 2 weeks, and two were sacrificed at 6 weeks after injections. The motor cortex from one 2-week monkey was not usable for immunohistochemistry and so this tissue was dropped from the study. Throughout the article this group of five monkeys will be referred to as the short survival group. Twenty-four *M. fascicularis* monkeys from an exercise study (Rhyu et al., 2010) were given 10 weekly injections of BrdU

TABLE 1.
Primary Antibodies Used for Immunohistochemistry

Antibody	Immunogen	Manufacturer catalog #, host species, mono- vs. polyclonal, and RRID #	Dilution used
Bromodeoxyuridine (BrdU)	BrdU incorporated into DNA	Accurate Chemical - AbD Serotec #T0030, rat monoclonal, RRID #AB609566	1:500
Calbindin (Cb)	Recombinant mouse calbindin	Chemicon-Millipore #AB1778, rabbit polyclonal, RRID #AB 2068348	1:200
Calretinin (Cr)	Recombinant rat calretinin	Chemicon-Millipore #AB5054, rabbit polyclonal, RRID #AB 2068506	1:500
Collagen IV (COL IV)	Collagen Type IV extracted and purified from mouse tumor	Chemicon-Millipore #AB756P, rabbit polyclonal, RRID #AB2276457	1:300
Doublecortin (DCx)	Synthetic peptide to human doublecortin corresponding to aa CysYLPLSLDDSD SLGDSM-free acid	Cell Signaling Technology #4604x, rabbit polyclonal, RRID # AB561007	1:400
Gamma amino butyric acid (GABA)	γ-aminobutyric acid (GABA) conjugated to BSA	Sigma-Aldridge #A2052, rabbit polyclonal, RRID #AB477652	1:2000
Glia fibrillary acidic protein (GFAP)	Purified bovine GFAP	Chemicon-Millipore #AB5804, Rabbit polyclonal, RRID #AB2109645	1:1600
Iba1 - (Ionized calcium binding adaptor molecule 1)	Synthetic peptide corresponding to C-terminus aa NA′-PTGPPAKKAISELP-C′	Wako Chemicals USA, Inc. #019-19741, rabbit polyclonal, RRID #AB839504	1:200
Neural-glial antibody 2 (NG2) 9.2.27	Human M14 melanoma cell extract	Gift from Dr. Ralph Reisfeld, Scripps Research Institute, mouse monoclonal	1:1500
Neuron specific nuclear protein (NeuN)	Purified cell nuclei from mouse brain	Chemicon-Millipore #AB377, mouse monoclonal, RRID # AB94966	1:500
Oligodendrocyte transcription factor 2 (Olig2) Rabbit anti-human	Synthetic peptide in portion of C-terminus of Human Olig2, aa 236-285	IBL-America #18953, rabbit polyclonal, RRID # AB494617	1:100
Platelet derived growth factor receptorß (PDGFrß)	Synthetic peptide, aa 1086-1106 from C-terminus of human PDGFrß	Epitomics -ABCAM #32570, rabbit monoclonal, RRID# AB777165.	1:400
S100ß	recombinant S-100ß	Swant 36 (discontinued),r bovine polyclonal	1:4000

(75 mg/kg) and sacrificed at 15 weeks (16 monkeys) or 27 weeks (8 monkeys) after initial BrdU injections to study the effects of age, exercise, postexercise inactivity, and longer survivals on the expression of BrdU and other antibody markers. Figure 1B summarizes the time line and experimental groupings of the exercise experiment. The monkeys were evenly divided into older (15–17 years) and younger (10–12 years) adults. Sixteen monkeys were trained to run on a treadmill 5 days a week for 9 weeks until they attained individual running speeds of 80% maximal aerobic power. These monkeys continued to run at optimal rates for an additional 15 weeks. Eight sedentary control monkeys sat on stationary treadmills during treadmill running sessions. Eight of the 16 running monkeys rested for an additional 12 weeks after exercise before they were killed. The monkeys of the experimental exercise study are referred to throughout the paper as the long survival monkeys.

Perfusion and tissue preparation

All monkeys were deeply anesthetized with sodium pentobarbital (30 mg/kg, i.v.) and perfused intracardially with physiological saline containing heparin (5000 U/l) and sodium nitrite (20 g/l) followed by cold 4% paraformaldehyde in PBS. The brain was removed and postfixed for 4 hours in cold 4% paraformaldehyde in phosphate-buffered saline (PBS) followed by immersion in 20% glycerol in PBS. The brains were cut into coronal blocks and placed in 30% sucrose in Tris-buffered saline (TBS) until sinking (~4 weeks with weekly change of solutions). Brain blocks containing the precentral gyrus (14 mm posterior to 7 mm anterior to the anterior commissure; Martin and Bowden, 2000) were covered with tissue freezing media, frozen at −19°C, and sectioned coronally at a thickness of 40 μm. Sections were collected in multiwell plates containing cryoprotectant (30% sucrose, 30% ethylene glycol in TBS) and stored at −20°C.

Fluorescence immunohistochemistry (IHC)

Free-floating sections of cortical tissue through the precentral gyrus and medial wall of the hemisphere to the cingulate fundus were processed for fluorescence IHC. Series of sections from every animal were batch-processed for combinations of antibody and lectin markers (Table 1). Control sections in each experiment underwent the same processing steps but were not incubated in primary antibodies. Tissue sections processed for BrdU and NG2 antibodies were washed in TBS then 0.6% H_2O_2 before incubating overnight at 4°C

in NG2 antibody alone or in combination with PDGFrβ antibody (see Table 1 for abbreviations). After washing in a solution of TBS and 0.5% Triton X in 3% normal donkey serum (TBS-TDS) for 1 hour at room temperature, sections were incubated in solutions of biotin-donkey-antimouse secondary antibody, ABC reagent, and tyramide (TSA)-Cy5 conjugate in amplification diluent (1:50 for 5 minutes). In tissue batches processed for both PDGFrβ and NG2 primary antibodies, fluorescein tagged donkey-antirabbit secondary antibody was added to the conjugated biotin secondary antibody solution. Following the first TSA amplification, sections were washed in TBS, then 0.6% H_2O_2, and then incubated in anti-fluorescein-horseradish peroxidase (HRP) conjugate for 30 minutes before the second TSA (TSA-Cy3). Following a TBS wash, sections were pretreated for BrdU processing in aqueous 2 N HCl for 30 minutes at 47°C followed by a neutralizing solution of 0.1 M boric acid in TBS (pH = 8.6) for 10 minutes at room temperature. Sections processed for collagen IV antibody were washed and incubated in a solution of pepsin (1 mg/ml) in .2 M HCl. After a 5-minute wash in TBS, nonspecific labeling was blocked by 0.5% Triton X and 3% normal donkey serum in TBS (TBS-NDS) for 1 hour at room temperature. Sections were incubated overnight at 4°C in anti-BrdU primary antibody, avidin blocking solution, and in some batches a second primary antibody. Following TBS-TDS and biotin blocking solution washes, sections were incubated in biotinylated donkey-antirat secondary antibody that was combined in some batches with other Cy3-conjugated secondary antibodies. Biotinylated antibody was visualized with Cy-2 conjugated streptavidin. Following TBS washes, some sections were incubated for 10 minutes at room temperature in *Lycopersicon esculentum* (tomato) lectin conjugated with Dylite 594. Sections were mounted on slides using Prolong Gold antifade mounting media (Molecular Probes, Eugene, OR).

Antibody characterization

Rat anti-BrdU antibody (clone BU1/75 [ICR1]), NeuN antibody for mature neurons, and DCx antibody for immature neurons were used on test sections through the motor cortex with sections from the hippocampus where new, immature, and mature neurons were known to exist (Kohler et al., 2011). $BrdU^-/NeuN^+$ expressing cells were pyramid-shaped or interneuron-like (determined by shape, size, and occasional colabeling with Cr antibody) and no labeling of glia or other cell types was observed. Manufacturer's data sheets indicate that NeuN antibody recognized 2–3 bands in the 46–48 kDa range and possibly another band at approximately western blot 66 kDa. Doublecortin antibody to the microtubule associated protein was characterized by western blot 45 kDa.

Calbindin (28 kDa) and calretinin (29 kDa) antibodies detect similar but distinct calcium binding proteins in interneurons. In our material, cells expressing these antibodies were predominantly bipolar and similar in size and morphology to Cr and Cb cell types described by others (Gabbott and Bacon, 1996; Barinka and Druga, 2010). Antibody to GABA also labeled cells that were similar in morphology, size, and location near large pyramidal cells to Cr-labeled interneurons. No other cell types were detected using these antibodies.

Iba antibody for microglia and s100β and GFAP antibodies for astrocytes were used to look for colabeling with NG2. Cells labeled with these antibodies were typical of microglia and astrocytes in the monkey cerebral cortex shown in a similar study by Koketsu et al. (2003). No other cell types were detected using these antibodies.

Col IV antibody recognizes the 139 kDa protein from mouse tumor tissue. Col IV is the collagen of basement membranes of brain pericytes. In our material, the antibody colocalized with NG2 labeling along vascular walls and defined both the luminal and abluminal membranes of $NG2^+$ cells. No other labeling with Col IV was observed.

Olig2 is a transcription factor for oligodendrocyte precursor cells that is localized in the nucleus but translocates to the cytoplasm in cells responding to brain injury (Cassiani-Ingoni et al., 2006). Olig2 colocalizes with NG2 in these cells (Ligon et al., 2006). In our material, Olig2 antibody only labeled nuclei of cells that were $NG2^+$.

We screened six NG2 antibodies in comparative IHC batches with rat and monkey brain sections. One NG2 antibody was Chemicon's (Temecula, CA) rabbit polyclonal (AB5320), and five antibodies, three rabbit polyclonals, and two mouse monoclonals were provided by Dr. William Stallcup. Only the mouse monoclonal antibody 9.2.27 demonstrated conclusively the presence of $NG2^+$ cells in monkey (but not in rat), whereas all polyclonal antibodies labeled $NG2^+$ cells in rat neocortex. NG2 polyclonal antibody 9.2.27 reacts with the core protein of chondroitin sulfate proteoglycan developed against human melanoma cells (Bumol et al., 1984). To our knowledge, this is the first reported study of $NG2^+$ cells in the brains of monkeys using this antibody.

PDGFrβ antibody recognizes the 190 kDa human platelet-derived growth factor, tyrosine kinase receptor. According to the product data sheet, this antibody does not crossreact with other CSF-1/PDGF receptor family members. In our material, PDGFrβ reacted with portions of all $NG2^+$ cells, but PDGFrβ and NG2 antibody

expression was not completely coincidental. No other cells were labeled with PDGFrβ antibody.

Quantification of new cells

Tissue sections from each animal were selected from randomly chosen wells for batch IHC. In most cases, the primary motor cortex from the cingulate to the central sulcus was dissected from the entire section to provide optimal staining of the greatest number of sections in the least amount of antibody. Two large IHC batches consisted of sections from the 24 long survival monkeys that stained for BrdU, NeuN, and Cr, or BrdU, NG2, and PDGFrβ. Smaller IHC batches combined sections from short and long survival monkeys so that batch effects of processing would be the same for both monkey groups. These batches were stained for BrdU, NG2, and either Cr, Olig2, or PDGFrβ. All short survival monkeys and all but one monkey (younger adult, control) from the long survival monkeys were sampled for counts of new $NG2^+$ cell phenotypes, and all monkeys from both groups were sampled for new Cr^+ cell counts. Counts of new cells stained for Olig2 and NG2 were made from four short survival monkeys and eight long survival, younger monkeys. Counts of new $PDGFr\beta^+$ cells were discontinued when it appeared that the antibody colabeled $NG2^+$ cells. Small IHC batches in 3–5 long survival monkeys were used to search for colabeling between antibodies to BrdU and DCx; BrdU, Col IV, and NG2; s100β and NG2; and Iba1 and NG2. No cells were counted in sections from these small IHC batches. In an initial count of $BrdU^+$, Cr^+, and $NeuN^+$ cells in 24 long survival monkeys, counts of 100 labeled cells / 3 sections/animal were made from three coronal sections through the precentral gyrus according to the rare event sampling protocol (Mouton, 2002). In subsequent IHC batches for Cr and other antibodies, fewer cells were counted (30–75/animal/IHC batch) from 3–5 sections per monkey. Small IHC batches were processed for GABA antibody to provide a comparison to Cr^+ cells. However, because cells labeled with GABA antibody might result from passive uptake rather than expression of the protein (Dayer et al., 2005), and because GABA antibody preparations are noisy compared to Cr antibody preparations, $GABA^+$ cells were not counted. Section slides were masked to obscure animal identities before labeled cells were imaged and counted using a Leica SP2 Confocal microscope (63× oil objective; 400× total magnification). The surface and white matter of the motor cortex of each section were outlined with a marker on the backs of the slides. After centering a slide, counting began by a zig-zag scan through the neocortex using a joystick to move the slide. Every new $BrdU^+$ cell was imaged and then recorded on an Excel spreadsheet. All images were reviewed off-scope to correct errors in data entry. Special images of cells with four labels were made using a Zeiss LSM 710 confocal microscope. Images were processed for publication using Leica LAF, Zeiss Zen, NIH ImageJ, and Canvas 8 and 11 softwares. Counts of new $NG2^+$ cell phenotypes of different morphologies, immunoreactivities, and relationships to other structures were totaled from IHC batches of short and long survival monkey tissue and estimates of phenotype proportions to total BrdU+ cells were made using binomial regression modeling. *P*-values were calculated for comparisons between groups of the exercise experiment using log odds ratios resulting from the binomial regression analysis.

RESULTS

It was clear from the first viewing of $NG2^+$ cells in the monkey motor cortex that these cells types displayed a variety of forms other than the polydendritic one that is used to commonly identify these cells (Nishiyama et al., 2009). In Figures 2–4, we illustrate $NG2^+$ cells in a progression of cell phenotypes from simple to complex. To determine if any of these cell types were responsive to the conditions of the study, we classified and counted new $NG2^+$ cells by their association with presumed vascular elements (perivascular, nonperivascular), the number and complexity of their cell processes (not multibranched, multibranched), and their colabeling with neuronal and glial antibodies. Counts of closely paired $BrdU^+/NG2^+$ cells were also made. In addition, we detected and counted a small proportion of new cells that expressed calretinin. We will first describe new cell phenotypes and then the proportions of new Cr^+ cells and $NG2^+$ cell phenotypes in short and long survival monkeys.

$NG2^+$ cell phenotypes

New, $NG2^+$ cells that merged with vessel walls and that lacked cell processes were classified as pericyte (Per) cells. We included cells with prominent $BrdU^+$ nuclei embedded in $NG2^+$-rich blood vessel walls (Fig. 2A) and cells on the abluminal surfaces of vessels (Fig. 2B–D). In some of the latter cell types, the cell membrane external to the nucleus was poorly labeled with NG2 (Fig. 2C) but the cell's basement membrane, a characteristic of pericytes (Krueger and Bechmann, 2010), could be identified by the presence of collagen IV external to the nucleus (2D). Furthermore, PDGFrβ, which is also characteristic of pericytes (Winkler et al., 2010), was found in these cells concentrated along the luminal membrane (Fig.

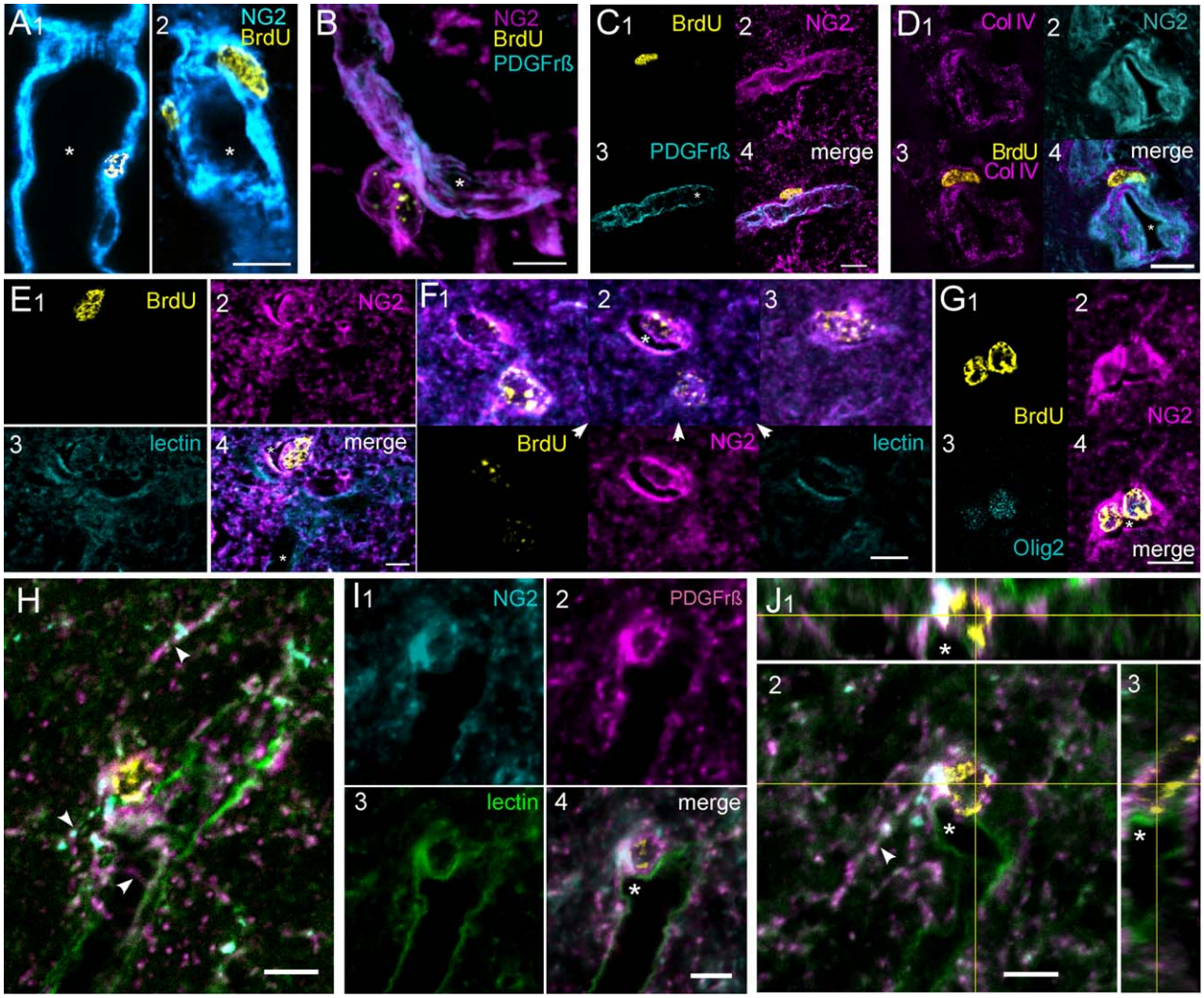

Figure 2. New NG2 cells classified as pericytes (A–D) and Elu cells (E–J). **A1,2:** New pericytes embedded in the walls of NG2-rich vessels. Cell processes of these cells are confined to the vessel walls. An unlabeled pericyte profile can be seen below the labeled cell in 1. Asterisks mark vessel lumens in this and other images of the figure. **B:** A new pericyte merges with the vessel wall. Longitudinal and transverse filaments in vessel wall typical of pericytes are highlighted by NG2 and PDGFrβ antibodies. **C:** New pericyte cell on vessel surface. PDGFrβ^{+} label is concentrated along the vessel lumen and transverse pericyte processes are visible. **D:** New pericyte on vessel surface lies internal to Col IV, a component of the basement membrane. **E:** Elu cell protruding into a small vascular space. The endothelial wall opposite the cell is labeled by tomato lectin. The vascular space was continuous with a larger, bifurcating vessel that would be invisible except for labeling of the vessel wall by tomato lectin. The vessel lumen is marked with an asterisk. **F:** Two Elu cells seen in three optical slices. Channels that make up the middle slice appear in the lower tier of images. The upper cell bulges into a small vascular space that is marked with tomato lectin. **G:** A pair of Elu cells labeled with Olig2. A small, branching process extends upward from the right cell. **H–J:** Three projection slices of an Elu cell at the branch point of a small vessel from a larger one (asterisk in I). Cell processes (arrowheads in H, J2) labeled with NG2 and PDGFrβ antibodies extend transversely and longitudinally along the vessel wall and into the brain parenchyma. PDGFrβ label was most concentrated next to the endothelial cell wall that is labeled with tomato lectin. Note that the nucleus of the cell is external to the endothelial wall. Three of four channels that make up merged images in H, I4, and J are shown in I1-3. J1, 3 are orthogonal images of J2. Scale bars = 10 μm.

2B,C). NG2 and PDGFrβ antibodies highlighted pericyte processes and longitudinal and transverse filaments of vessel walls (Fig. 2A–C). Per cells were found in monkeys that survived 2 days following a single BrdU injection and in animals that survived 27 weeks after the initial injection of 10 weekly BrdU injections.

A second type of BrdU^{+}/NG2^{+} cell lacked clearly defined cell processes (Fig. 2E,F) or had few, simply branched ones that followed vessel walls or extended short distances into the parenchyma (Fig. 2G–J). Because of their simple form and association with vascular elements, these cells were counted with Per cells as a single category. The cell body of these cells protruded into

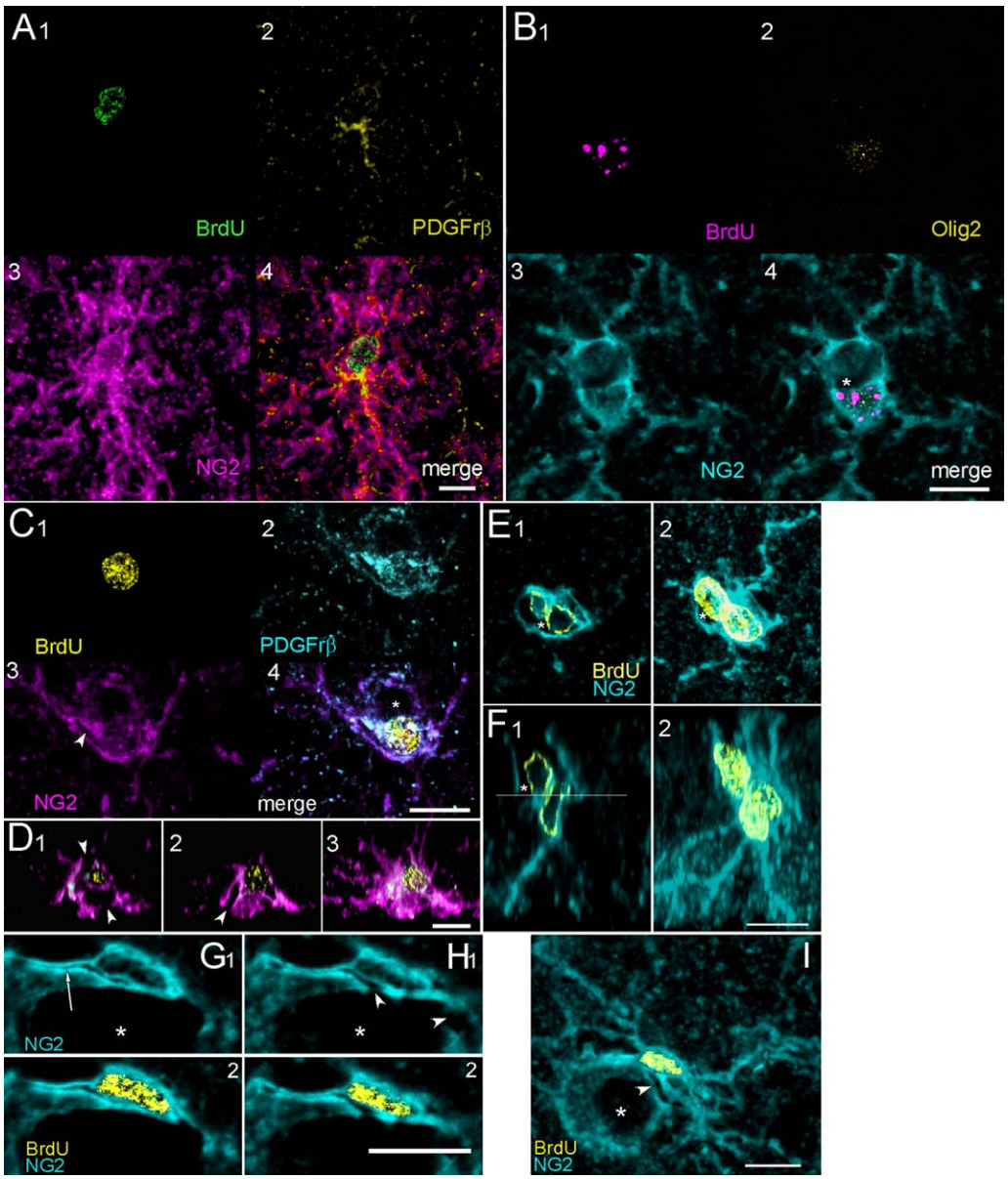

Figure 3. Polydendrocytes (Pld) and polydendritic perivascular cells (Pldv) are characterized by multiple, complex branches. **A:** A pair of new Pld cells with closely paired nuclei indicating recent cell division. PDGFrβ labeling was seen near the cell body and in one process of the lower cell but these cells were not perivascular. **B:** Two Pldv cells with thick, branching dendrites enclosing a small vascular space (asterisk). Only the lower cell is new born and sparsely labeled with Olig2. **C,D:** A new Pldv cell partially enclosing a small vessel (**C4**, asterisk; arrowheads in **C3** and orthogonal slices **D1,2**). The projection stack of sections in **D3** shows multiple branching processes of the cell that obscure the vessel. **E,F:** A pair of Pldv cells and adjacent vessel shown in two slice planes. The vessel lumen (asterisks) can be seen in single sections (**E1,F1**) but is obscured by the processes of the cell in maximum projection stacks (**E2,F2**). The approximate plane of section for **E1** can be seen as line in **F1**. **G–I:** A Pldv cell with unstained passage (arrow) in a cell process extending to the left and clefts (arrowheads) that are continuous with adjacent vessel. **G–H:** Two optical slices through the cell showing NG2 and combined BrdU and NG2 channels. **I:** A z projection stack of all optical slices through the cell. The arrowhead points to a cleft that opens into the lumen of the vessel seen in **H1**. Scale bars = 10 μm.

the small vessels where they were located and cytoplasmic extensions from the cells partially enclosed vascular spaces. In some examples, we confirmed the presence of vessel walls using tomato lectin (Fig. 2E–J) (Porter et al., 1990). We called these $NG2^+$ cells early lumen (Elu) cells because they appeared at sites of small vessel branches (Fig. 2I). Expression of PDGFrβ in Elu cells was concentrated along the vessel wall, but other parts of the cell, including processes, displayed patches of PDGFrβ marker (Fig. 2H,J).

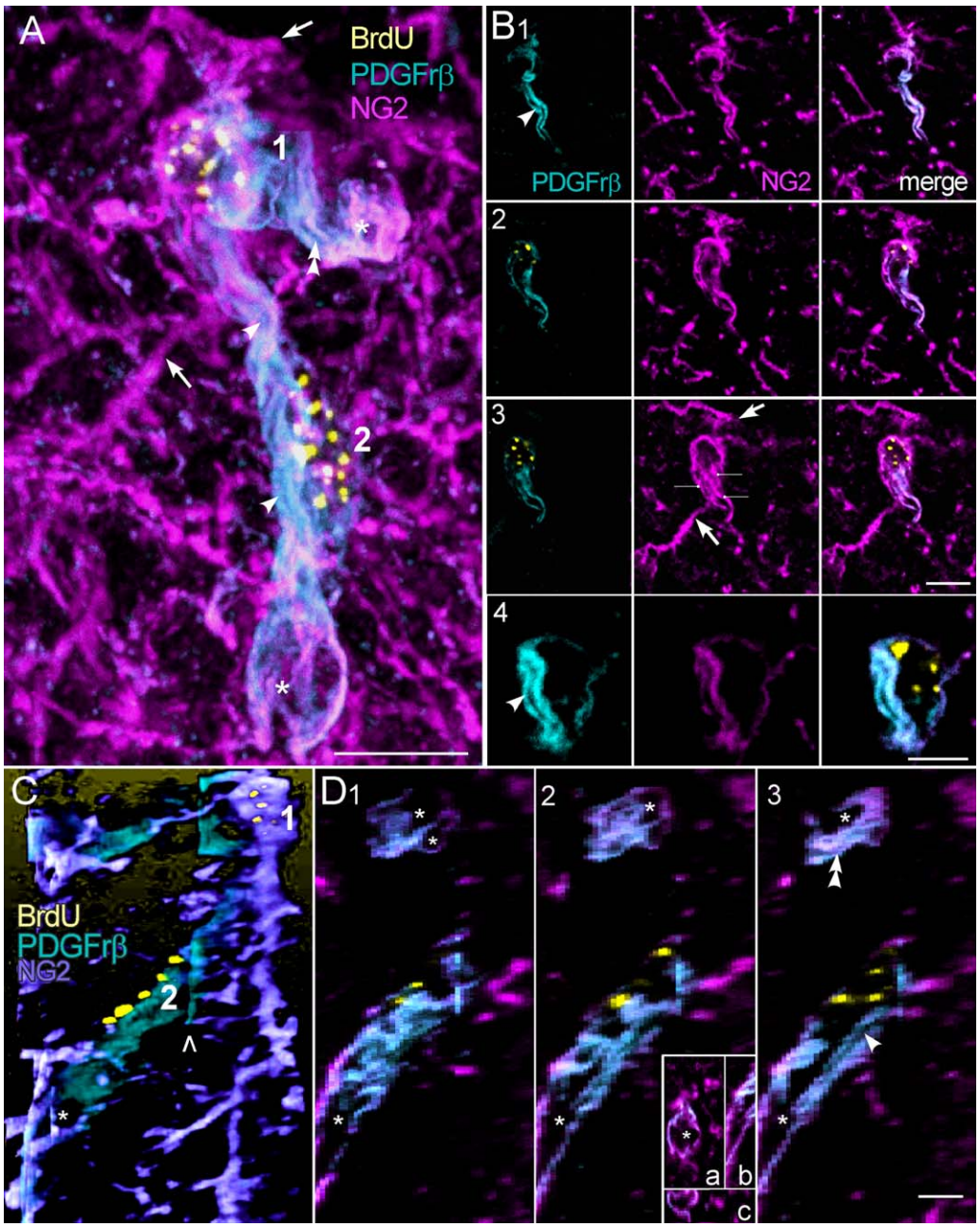

Figure 4. Two NG2$^+$ cells showing vacuoles and tube-like passages within processes labeled with PDGFrβ antibody. **A:** A merged, projection stack image of the cells (1,2). Two of many NG2$^+$- rich processes that have little or no PDGFrβ$^+$ are marked with arrows (also in **B3)**. Two processes are densely colabeled with PDGFrβ$^+$ and contain tube-like passages (single and double arrowheads; also in **B1,4**; **D3**) that extend the length of the processes and end in large expansions (asterisks). The large, central process appears to be a complex of processes from cells 1 and 2, whereas the shorter, horizontal process arises from cell 1 alone. **B1–4**: Single xy slices, showing a central passage (arrowheads) extending between the perinuclear regions of cells 1 and 2. Note the budding of a tube-like passage in the horizontal process in **B1**. Smaller vacuoles are seen in **B2**. **C:** Side view reconstruction of the two cells showing the two PDGFrβ-labeled processes (other processes were digitally removed). The open arrowhead shows an alignment artifact (also seen in **D1–3**) between the two stacks that make up images **A** and **C**. **D1–3**: Single yz slices showing the central (arrowhead) and horizontal (double arrowheads) passages seen in **A**. The central tube ends in an expansion (asterisks). The inset in 2 shows the expansion in optical slices that are adjacent to the one in 2 (a, xy; b, yz; c, xz slice planes). Note that the expansion is enclosed within the process. Scale bars = 10 μm.

Cells with multiple branched processes characterized a common type of BrdU$^+$/NG2$^+$ cell. In rodents, these cells are identified as polydendrocytes (Nishiyama et al., 2009) and we adopted this terminology. In the macaque, the characteristic processes of polydendritic (Pld) cells are irregular, tortuous branches radiating as

TABLE 2.
Cell Pairs

Monkey	BrdU#	% BrdU
2 d	80	36
2 d	46	15
2 w	66	15
6 w	75	11
6 w	79	06
mean/SEM		17 ± 5
OR	34	09
YC	31	06
YR	30	10
YRS	18	05
YRS	40	03
mean/SEM		07 ± 1

Percentages of $BrdU^+$ cell pairs with respect to BrdU cell totals from a single IHC batch that processed sections for BrdU, NG2, and Olig2 antibodies using tissue from monkeys with single BrdU injections and short survivals after BrdU (top) and monkeys with multiple BrdU injections and long survivals after BrdU (bottom). 2 d, 2 day; 2 w, 2 week; 6 w, 6 week; OR, Older runners, YC, younger controls, YR, younger runners, YRS, younger run-stops.

far as 35 μm from the cell body and frequently intertwining (Fig. 3). The processes varied. In some cells they were thin and relatively uniform in diameter, but in others they appeared more varicose. When these cells were found apart from vascular structures, they were counted as a separate population of $NG2^+$ cells (Fig. 3A). However, we also found a perivascular subtype of Pld cells that we counted as Pldv cells. Like Elu cells, Pldv cells partially enclosed vascular spaces and Pldv cell bodies protruded into those spaces (Fig. 3B–**I**), but Pldv cells had multibranched processes that often obscured the vessel lumen that they bordered (Fig. 3D3,E2,F2). Unlike Pld cells, that tended to be more uniformly spaced in the parenchyma, pairs of Pldv cells formed complex structures along vessel walls (Figs. 3B,E,F, 4). Unstained clefts in the cell body of Pldv cells appeared to be continuous with adjacent blood vessels (Fig. 3C,D,**G–I**), and unstained vacuoles and narrow passages in the cytoplasm (Fig. 3**G–I**) localized in some cell processes but not others. The last named features are shown in greater detail in a complex of two Pld cells in Figure 4. Only two of the multiple $NG2^+$ labeled processes from these cells express PDGFrβ and contain tube-like passages (single and double arrowheads) that end in large vacuolar expansions (Fig. 4A,C,D; asterisks). The passages appear to be enclosed by longitudinal filaments, possibly actin filament bundles, that labeled with NG2 and PDGFrβ antibodies (Fig. 4A,B3; lines). The large, central process appears to be a complex of processes from cells 1 and 2, whereas the shorter process is oriented nearly perpendicular to the longer one and arises from cell 1 alone. The clumped $BrdU^+$ chromatin in both cells is indicative of late S stage in the cell cycle (Chagin et al., 2010) and the differential distribution of PDGFrβ suggests asymmetry in the subsequent cell divisions.

$BrdU^+/NG2^+$ cell pairs

Counts were made of closely spaced pairs of $BrdU^+/NG2^+$ cells that, by their appearance within the same image frame, suggested recent cell division. Cell pairs were most common in monkeys with short post-BrdU survival periods of 2 weeks or less (36% and 15% at 2 days; 15% at 2 weeks) but by 6 weeks after BrdU injection, there were fewer new cell pairs (11% and 6%). The mean and SEM for all new $NG2^+$ cell pairs in the short survival monkeys was 17% ± 5% (Table 2, top). In monkeys with longer post-BrdU survival times, pairs of $BrdU^+/NG2^+$ cell counts ranged from 2.5% to 10% of total $BrdU^+$ cells (mean, 7% ± 1%) (Table 2, bottom). $BrdU^+/NG2^+$ cell pairs were found as simple Per and Elu, cells (Fig. 2F,G) and multibranched Pld and Pldv cells (Fig. 3A,E).

Neuronal phenotypes

We used antibodies to neuronal proteins NeuN, Cr, GABA, Cb, and DCx, in combination with BrdU antibody to look for the presence of new neurons in the precentral gyrus. Because no colabeling with DCx or Cb antibodies was seen in low-magnification scans, we discontinued use of these antibodies. $BrdU^+/Cr^+$ cells were found but most of these cells were weakly labeled compared to nearby $BrdU^-/Cr^+$ cells. Only about 25% of Cr^+ cells had well-developed processes (Fig. 5A,B) and denser Cr^+ labeling. $BrdU^+/GABA^+$ cells were also found that were similar to Cr^+ cells in size and juxtaposition to larger neurons (Fig. 5C). $BrdU^-/Cr^+$ cells colabeled with NeuN antibody (Fig. 5D) but no new Cr^+ or $GABA^+$ cells were $NeuN^+$. About 7.5% (181/2400) of new cells were Cr^+ in a sampling of 100 cells from each of 24 experimental monkeys, and almost half of these cells (48%) were found in eight run-stop monkeys that survived the longest period after multiple BrdU injections. In a second study, brain sections from five monkeys with short, post-BrdU survivals and four run-stop monkeys with 27-week, post-BrdU survivals were processed with BrdU, Cr, and NG2 antibodies. We found a comparable percentage of $BrdU^+/Cr^+$ cells (~7.6%, $n = 383$) as in the first study. Also similar to the results in the first study, there were almost 5 times as many $BrdU^+/Cr^+$ cells in the run-stop group of monkeys. Satellite $BrdU^+/Cr^+$, $BrdU^-/Cr^+$, and $BrdU^+/GABA^+$ cells were often found in close apposition to the soma of larger $NeuN^+$ neurons (Fig. 5B–D) and, occasionally, we saw satellite $NG2^+$ cells with unstained profiles of large pyramids (not shown) but a

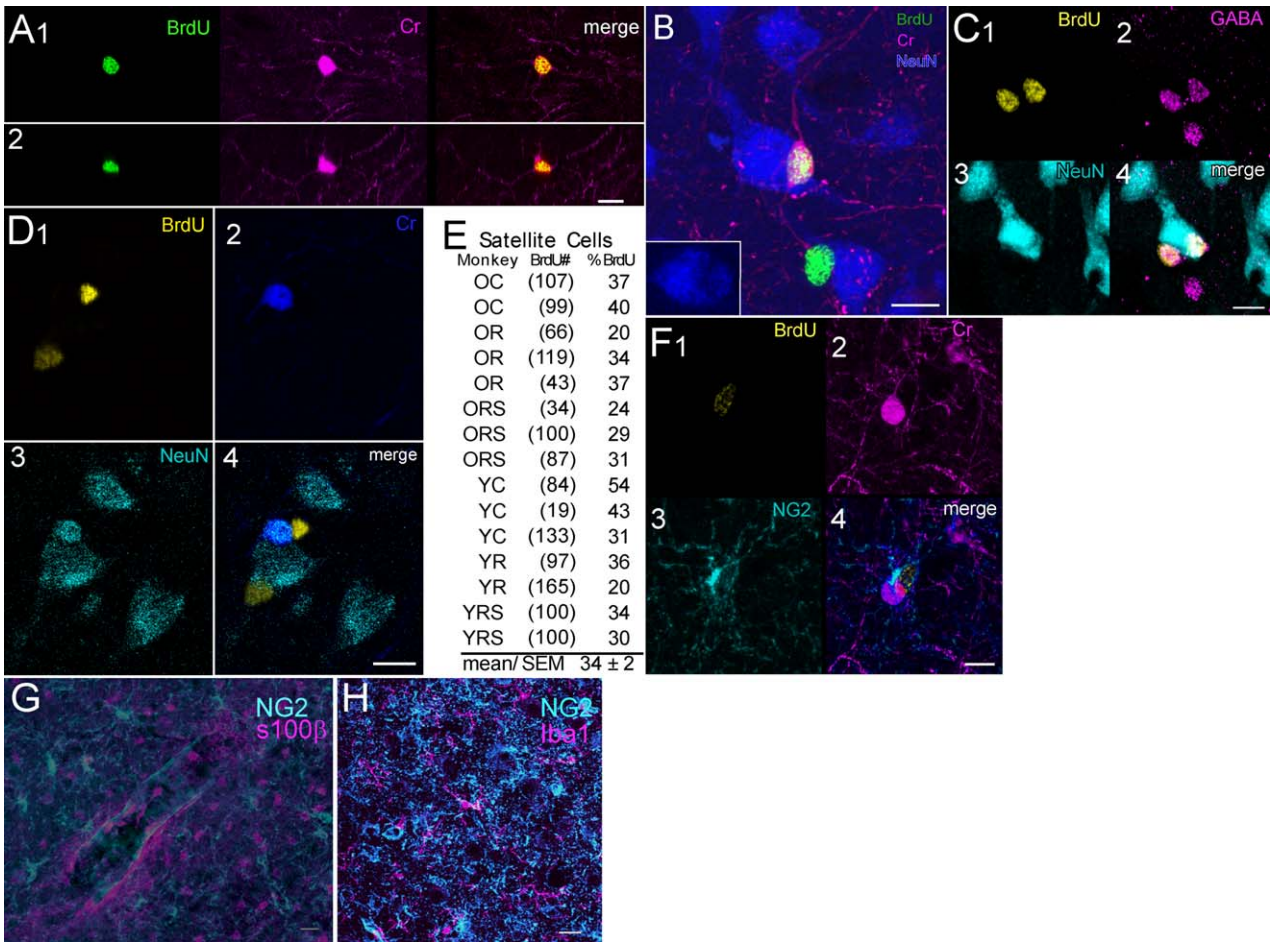

Figure 5. BrdU$^+$ cells labeled with Cr, GABA, and glial antibodies. **A:** Single optical sections in the xy and xz planes through a multipolar BrdU$^+$/Cr$^+$ cell. **B:** A bipolar, BrdU$^+$/Cr$^+$ cell and single-labeled BrdU$^+$ cell. The bipolar cell is closely apposed to the larger NeuN$^+$ neuron. Inset shows the impression made by the Cr$^+$ cell. **C:** Two BrdU$^+$/GABA$^+$ satellite cells juxtaposed on a larger NeuN neuron. A third, BrdU$^-$/GABA$^+$ cell is also seen. Note all GABA$^+$ cells are immature but are comparable in size and in juxtaneuronal position to the Cr$^+$ cell seen in B. **D:** Two BrdU$^+$ neurons that are satellite cells on NeuN$^+$ and NeuN$^+$/Cr$^+$ cells. **E:** Percentages of BrdU$^+$ counted as neuronal satellites in a series of exercise monkeys. OC, older control; OR, older runner; ORS, older run-stop; YC, younger control; YR, younger runner; YRS, younger run-stop. **F:** BrdU$^+$/NG2$^+$ cell closely applied to a Cr$^+$ cell. **G:** NG2 and s100β antibodies label separate populations of cells. **H:** NG2 and Iba1 label separate populations of cells. Scale bars = 10 μm.

separate count of satellite phenotypes was not made. New NG2$^+$ cells were also seen juxtaposed onto BrdU$^-$/Cr$^+$ cells (Fig. 5F) but not BrdU$^+$/Cr$^+$ cells and no NG2$^+$ cells colabeled with Cr antibody. In a count of monkeys from the six groups of the exercise study, we estimated about 34% (SEM ± 2%) of BrdU$^+$ cells were satellite cells on NeuN$^+$ neurons (Fig. 5E).

Other glial markers

Low-magnification, confocal microscope scans were used to look for colabeling of microglial antibody Iba1 and astrocyte antibodies GFAP and s100β with NG2$^+$ cells. NG2$^+$ cells were morphologically distinct from astrocytes and microglia and no cells were double-labeled. (Fig. 5G,H). Therefore, we discontinued use of s100β and IBa4 antibodies. The oligodendrocyte cell line protein, Olig2, was expressed in about 78% of BrdU$^+$/NG2$^+$ cells (SEM ± 4%; n = 375 cells) in one IHC batch. The granular, nuclear labeling with Olig2 antibody was easily detectable in some NeuN$^+$ cells (Fig. 2G) but very sparse or not detectable in others (Fig. 3B). In all cases, Olig2 labeling was confined to the nucleus and no cells were Olig2$^+$/NG2$^-$. Except for Per cells, all other NG2$^+$ cell phenotypes expressed Olig2.

Unidentified cells

BrdU$^+$/NG2$^+$ cells that were not multibranched and not perivascular were classified as NG2$^+$ unknown cells in Tables 3 and 4. New cells that did not express NG2

TABLE 3.

New Cell Phenotypes in Monkeys With Short Survivals After Single BrdU Injections

A.

Post-Brdu survival *(BrdU #)*	$NG2^+$ cells				$NG2^-$ cells		Combined cell types				
	Per-Elu	Pldv	Pld	$NG2^+$ unk[a]	perivasc	NOT perivasc	Total $NG2^+$	All $NG2^+$ perivasc[b]	All perivasc[c]	$NG2^+$ multi-branch[d]	$NG2^+$ NOT multi-branch[e]
2 d *(121)*	43 *(52)*	5 *(6)*	18 *(22)*	28 *(34)*	1 *(1)*	6 *(6)*	94 *(114)*	48	49	23	71
2 d *(92)*	40 *(37)*	0 *(0)*	10 *(9)*	40 *(37)*	3 *(3)*	7 *(6)*	90 *(83)*	40	43	10	80
2 w *(109)*	48 *(52)*	6 *(7)*	21 *(23)*	8 *(9)*	5 *(5)*	13 *(14)*	83 *(91)*	54	59	28	56
6 w *(115)*	16 *(18)*	29 *(33)*	34 *(39)*	9 *(10)*	3 *(4)*	10 *(11)*	86 *(99)*	44	48	63	24
6 w *(119)*	22 *(26)*	13 *(16)*	34 *(41)*	6 *(7)*	3 *(3)*	19 *(23)*	74 *(88)*	35	38	48	28

B.

Cell type or combination	Lower	Estimate	Upper
All NG2/BrdU	83	86	89
Per-Elu	29	33	37
Pldv	9	11	14
Pld	21	24	28
$NG2^+$ unknown	14	17	21
$NG2^-$ perivascular	2	3	5
$NG2^-$ NOT perivascular	9	11	14
$NG2^+$ perivascular combined	40	44	48
All perivascular	43	47	52
$NG2^+$ Multi-branched	31	35	39
$NG2^+$ NOT Multi-branched	46	51	55

A: Percentages of $BrdU^+$ cell totals for $NG2^+$ and $NG2^-$ cell types and cell combinations from monkeys with single BrdU injections and short survivals after BrdU. Cell counts are in parentheses and italicized. 2 d, 2 day; 2 w, 2 week; 6 w, 6 week; a, $NG2^+$ unknown (not perivascular, not multi-branched); b, Per-Elu and Pldv; c, Per-Elu, Pldv, and $NG2^-$ perivascular; d, Pldv and Pld; e, Per-Elu, and $NG2^+$ unk. B: Estimated mean percentages and ranges of new cell phenotypes and combinations based on binomial regression modeling.

TABLE 4.

New Cell Phenotypes in Monkeys With Long Survivals After Multiple BrdU Injections

A.

Cell type or combination	Lower	Estimate	Upper
All NG2%BrdU	83%	85%	87%
PerElu	24%	27%	30%
Pldv	20%	23%	26%
Pld	25%	27%	30%
$NG2^+$ unknown	5%	7%	8%
$NG2^-$ perivascular	3%	4%	5%
$NG2^-$ NOT perivascular	9%	11%	13%
$NG2^+$ perivascular combined	48%	51%	54%
All perivascular	51%	54%	57%
Multibranched	48%	51%	54%
NOT Multibranched	31%	34%	37%

B.

	$NG2^+$ cells				$NG2^-$ cells		Combined cell types				
Group (BrdU#)	Per-Elu	Pldv	Pld	$NG2^+$ unk	perivasc.	NOT perivasc.	Total $NG2^+$	All $NG2^+$ perivasc.	All perivasc.	$NG2^+$ Multi-branch	$NG2^+$ NOT multi-branch
OC *(136)*	26 ± 8 *(35)*	39 ± 10 *(53)*	21 ± 8 *(28)*	6 ± 1 (8)	3 ± 2 *(4)*	6 ± 3 *(8)*	91 ± 3 *(124)*	65 ± 6	68 ± 7	60 ± 11	32 ± 8
OR *(185)*	34 ± 4 *(62)*	19 ± 2 *(35)*	25 ± 4 *(46)*	8 ± 4 *(14)*	3 ± 2 *(6)*	12 ± 5 *(22)*	85 ± 3 *(157)*	52 ± 5	56 ± 4	44 ± 3	41 ± 3
ORS *(154)*	32 ± 6 *(50)*	21 ± 7 *(32)*	21 ± 13 *(33)*	10 ± 4 *(16)*	5 ± 1 *(8)*	10 ± 4 *(15)*	85 ± 3 *(131)*	53 ± 2	58 ± 3	42 ± 13	43 ± 9
YC *(84)*	30 ± 12 *(25)*	19 ± 8 *(16)*	32 ± 10 *(27)*	2 ± 1 *(2)*	5 ± 4 *(4)*	12 ± 3 *(10)*	83 ± 2 *(70)*	49 ± 3	54 ± 8	51 ± 14	32 ± 14
YR *(204)*	21 ± 3 *(42)*	30 ± 5 *(61)*	33 ± 6 *(68)*	5 ± 2 *(10)*	4 ± 2 *(8)*	7 ± 2 *(15)*	89 ± 3 *(181)*	50 ± 3	54 ± 2	50 ± 10	25 ± 6
YRS *(376)*	24 ± 5 *(92)*	13 ± 3 *(48)*	31 ± 3 *(115)*	10 ± 2 *(36)*	3 ± 2 *(10)*	20 ± 4 *(75)*	77 ± 4 *(291)*	37 ± 6	40 ± 6	37 ± 3	34 ± 6
Comparisons						*P* values					
OC - OR		**								*	–
OC - ORS		*								*	
OC - YC		*									
OC - YRS		**				**	**	**	**	*	–
OR - YR										**	–
OR - YRS	*										
ORS – YR										**	
YR - YRS							*	*	*	**	–
YRS – ORS								**	**		
All Run-stops v All Controls		**		*		*	*	**	**	**	–
All Runners v All Controls											–
All Runners v All Run-stops						**	*	*	*	**	–

A: Estimated mean percentages and ranges for new cell phenotypes and cell combinations based on binomial regression modeling. B: Above, mean percentages of $BrdU^+$ cell totals and SEMs for $NG2^+$ and $NG2^-$ cell types and cell combinations from each group of experimental exercise monkeys. Cell counts are in parentheses and italicized. Below, *P* values of significant differences in paired comparisons of exercise groups. Calculated *P*-values correspond to comparing the log odds ratios resulting from binomial regression analysis.

*$P = 0.05 - 0.01$;

**$P > 0.01$. OC, older control group; OR, older runner group; ORS, older run-stop group; YC, younger control group; YR, younger runner group; YRS, younger run-stop group; $n = 4$ except YC where $n = 3$.

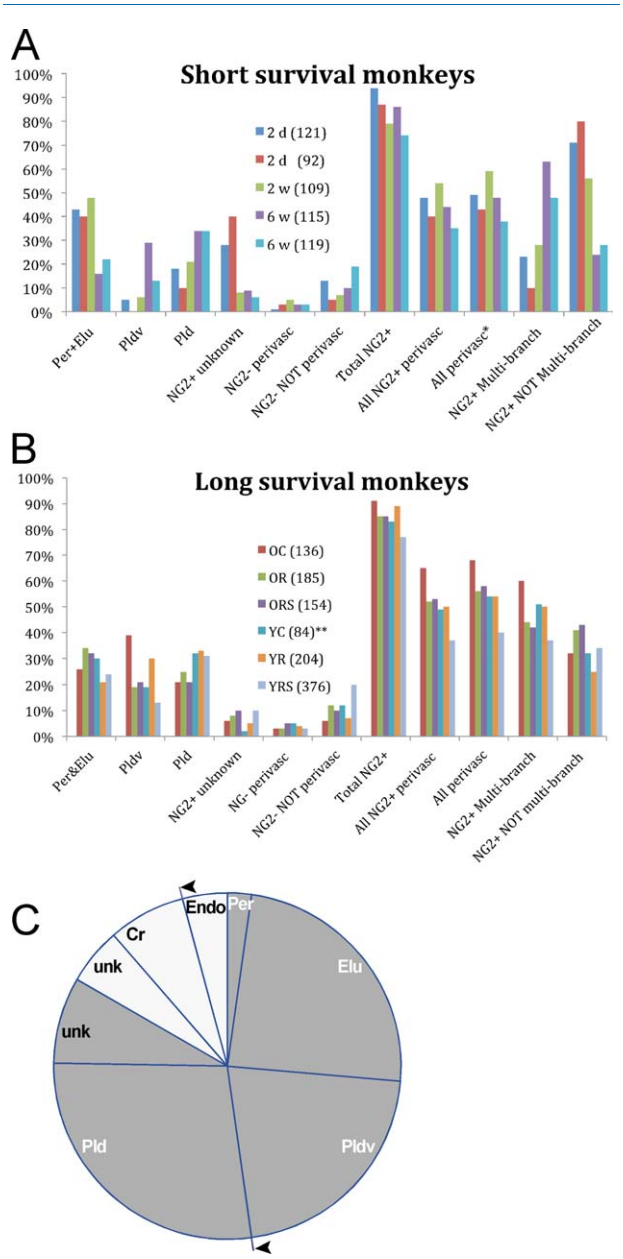

Figure 6. **A:** Estimated mean percentages, relative to $BrdU^+$ cell totals, of individual and combined $NG2^+$ and $NG2^-$ cell types from monkeys that survived short periods after single BrdU injections. **B:** Estimated mean percentages of individual and combined $NG2^+$ and $NG2^-$ cell types from monkeys that survived long periods after multiple BrdU injections. **C:** Relative proportions of adult born ($BrdU^+$) cell types defined morphologically and immunohistochemically. The cumulative means listed in Table 2 were used to construct proportionate wedges of the chart. $BrdU^+/NG2^+$ cells are represented by gray wedges. Per cells (2.5%) are shown separately from the Per-Elu group. $BrdU^+/NG2^-$ cells (perivascular, non-perivascular) appear as white wedges with a separate wedge for Cr^+ cells (7–8%) derived from the total non-perivascular group in Table 2. All adult born perivascular cells appear in wedge segments between the arrowheads. Satellite cells comprising about 34% of all $BrdU^+$ cells are not shown. $NG2^+$ unk: unknown, not perivascular, not multibranched new cells; $NG2^-$ unk: not perivascular new cells.

($NG2^-$) were counted as perivascular or not perivascular. Based on morphology and cell location, we reasoned that some $BrdU^+/NG2^-$ perivascular cells were endothelial cells or mature pericytes that no longer expressed NG2. The cell group, $BrdU^+/NG2^-$ NOT perivascular, included $BrdU^+/Cr^+$ cells.

Cell phenotype proportions: single injection, short survival monkeys

The percentages of $BrdU^+$ cell totals for all $NG2^+$ cells, individual cell types, and cell combinations in the five monkeys that survived 2 days, 2 weeks, and 6 weeks following single BrdU injections appear in Table 3 and Figure 6A. Per and Elu cells were counted as a single category for the analysis. The data in Table 3A shows reciprocal trends in $NG2^+$ cell branch morphology with respect to time after BrdU injections. Percentages of $NG2^+$ cells with few or no processes (Per-Elu, $NG2^+$ unknown) were high in monkeys that survived 2 days and 2 weeks and one-third to one-half lower in monkeys that survived 6 weeks, whereas the percentages of multibranched cells (Pldv, Pld) were higher in the monkeys that survived 6 weeks after single BrdU injections and much lower in monkeys that survived 2 days and 2 weeks. Furthermore, percentages of unidentified $NG2^+$ cells ($NG2^+$ unknown) cells were 3–6 times higher in monkeys with 2-day survivals than in monkeys with survivals of 2 or 6 weeks. The estimated means for total $NG2^+$ cells and cell types appears in Table 3B. About 86% of total $BrdU^+$ cells counted ($n = 556$) were $NG2^+$, of which 47% were all perivascular (sum of Per-Elu, Pldv, $NG2^-$ perivascular). In short survival monkeys, Cr^+ cells comprised about 10% of the category $NG2^-$ NOT-perivascular cells.

Cell phenotype proportions: multiple injection, long survival monkeys

Estimated mean percentages of $BrdU^+$ cell totals for individual cell types and cell combinations from experimental exercise monkeys with multiple BrdU injections and long post-BrdU survivals are shown in Table 4 and Figure 6B. The estimated percentage of all $NG2^+$ cells was about 85% (Table 4A) as compared to 86% (Table 3B) in short survival monkeys. Percentages of individual cell types overlapped upper and lower estimates between the two datasets except for Pldv and $NG2^+$ unknown cells. The respective increase and decrease in percentages of these two cell types in experimental animals were attributed to maturation from simple to complex branching forms that appeared to occur around 6 weeks after BrdU injections. (Note that the mean percentage of Pldv cells from the two 6-week monkeys

was 21% (Table 3B), compared to a mean of 22% for Pldv cells from experimental animals (Table 4A).) The higher Pldv cell percentages in long survival monkeys weighted the percentages of multibranched cells, $NG2^+$ perivascular cells, and all perivascular cells in this group relative to the short survival monkeys, but the percentages of Pld cells in the two groups largely overlapped. One unseen difference in the two datasets was in the percentages of $BrdU^+/NG2^-$ cells. This cell category contained cells that were unidentified in monkeys with short post-BrdU injection survivals but in monkeys with longer survival times after BrdU, this category included Cr^+ cells. In long survival monkeys, Cr^+ cells made up about one-third of the total $NG2^-$ nonperivascular cells and about half of these cells were counted in younger run-stop (YRS) monkeys.

Table 4B shows the percentages of $BrdU^+$ cell totals for individual cell types and cell combinations from each experimental exercise group. Pairwise comparisons were made between each group for each cell type and cell combination. Significant comparisons (lower part of the table) were influenced by the following outcomes. 1) Older control (OC) monkeys had the highest percentage of Pldv cells and Total $NG2^+$ cells. The percentage of Pldv cells in OC group was significantly higher than the percentage of this cell type in other groups except younger runners and the high percentage of Pldv cells probably contributed to the significant difference in the combined group comparison of All controls versus All Run-stops. 2) The YRS group had the lowest percentage of Pldv cells and the lowest percentages of cells in the Total $NG2^+$, All $NG2^+$ perivascular, All perivascular, and $NG2^+$ multibranched cell categories. The percentages of cells in these categories were significantly lower in YRS monkeys compared to YR monkeys and in All Run-stop versus All Runner monkeys, which suggested a possible effect of the postexercise sedentary period. 3) YRS monkeys had the highest percentage of $BrdU^+/NG2^-$, NOT perivascular cells, which contributed to a statistically significant difference in the comparison of this cell category between All Run-stops and All Runners and All Run-stops and Controls. 4) ORS and YRS monkeys had the highest percentages of $NG2^+$ unknown cells (not multibranched, not perivascular), which contributed to a statistically significant difference in the comparison of this cell category between All Run-stops and All Controls. The last two comparisons suggest that unidentified new cells increase during the postexercise period. A significant age-related comparison of individual $NG2^+$ cells types was the higher percentage of Per-Elu cells in the OR group versus the YR group, whereas the OR monkeys had a lower percentage of $NG2^+$ multibranched cells. The ORS group also had a significantly higher percentage of $NG2^+$ perivascular and All perivascular cell combinations compared to the YRS group. No other individual cell type comparisons were significantly different between groups and no significant differences were seen in any cell type category between all runners and all controls.

Cell type summary

The relative proportions of adult born cell types that were morphologically and immunohistochemically identified in the present study are summarized in Fig. 6C using data from Table 4A. A little more than half (~54%) of $BrdU^+$ cells are perivascular including probable pericytes, two $NG2^+$ cell types (Elu, Pldv) that have not been described previously, and $NG2^-$ perivascular cells that include possible endothelial cells and mature pericytes. We estimated that about 2.5% ($n = 722$, SEM $<1\%$) of BrdU cells from three IHC batches were Per-type cells. Calretinin-labeled $BrdU^+$ cells were separated from other $NG2^-$ nonperivascular cells. An estimated 34% of BrdU cells are neuronal satellite cells that are not represented in the chart.

DISCUSSION

Perivascular progenitor cells

The major finding of this study is that nearly half of $BrdU^+/NG2^+$ cells are structurally and immunohistochemically associated with blood vessels in the motor cortex of adult macaque monkeys. This is the largest group of $BrdU^+/NG2^+$ cells that comprise 86% of adult born cells. Another 3–4% of $BrdU^+/NG2^-$ cells were found in and on vessel walls and probably included some endothelial and mature pericytes cells that do not label with NG2 antibody. Therefore, during the post-BrdU administration time periods that we studied, up to 54% of new cells were perivascular in monkeys that survived the longest periods after BrdU injections.

The perivascular niche where $NG2^+$ perivascular cells are found is a region of local cell proliferation, differentiation, and remodeling in the brain and other tissues (Diaz-Flores et al., 2009; Dore-Duffy and Cleary, 2011; Paul et al., 2012). In the brain, cell signaling between endothelial cells and nearby cells of the parenchyma has been linked to neurogenesis in the hippocampus of rats (Palmer et al., 2000), oligodendrocyte-induced vascular remodeling in the injured mouse corpus callosum (Pham et al., 2012), and pericyte activity during angiogenic responses to injury (Diaz-Flores et al., 2009; Goritz et al., 2011) or hypoxia in mice (Dore-Duffy and LaManna, 2007). In particular, PDGF-B/PDGFrβ signaling between endothelial cells and pericytes plays a

major role in developmental angiogenesis (Ozerdem et al., 2001) and maintenance of adult microvasculature (Bell et al., 2010). In the present study we show examples of Per, Elu, and Pldv cells labeled with PDGFrβ antibody along endothelial walls like that shown by Ozerdem et al. (2001) and Bell et al. (2010). We also found PDGFrβ antibody expression in selected processes of Pld cells that coincided with the formation of tube-like passages by cytoskeletal filaments. It is quite possible that some of these cytoskeletal filaments are actin filament bundles that colocalize and interact with NG2 to effect cytoskeletal rearrangements such as those that promote motility of cells (Fang et al., 1999) and cell processes (Haberlandt et al., 2011). Actin, NG2, and PDGFrβ$^+$ also colocalize in pericytes of the retina and choroid (Trost et al., 2013) and in mobilized A type pericytes of the injured spinal cord (Goritz et al., 2011). The long tube-like passages in Pld cells also resemble the PDGFrβ-enriched tubes of embryonic pericytes (Ozerdem et al., 2001; Virgintino et al., 2007) that serve as prevascular scaffolding for later endothelial cell investment. The similarities to pericytes in appearance suggest the possibility that some Elu and Pldv cells might be incorporated into vessel walls at small vessel branch points in the presence of existing endothelial cells or, in the case of Pld cells with tube-like passages, might provide a prevascular framework for endothelial cell wall formation. These two models of vessel formation would be expected to yield vessels of different form and dynamics.

NG2 cell maturation

The possibility that some perivascular NG2$^+$ cells might have pericyte-like functions or even become pericytes does not conflict with the idea that most NG2$^+$ cells are oligodendrocyte precursor cells (Dawson et al., 2003; Dimou et al., 2008; Kang et al., 2010; Simon et al., 2011; Hughes et al., 2013). We made several observations that support this idea. First, a large percentage of NG2$^+$ cells (78%) colabeled with Olig2, a transcription protein vital for maturation of oligodendrocytes (Ligon et al., 2006). All BrdU$^+$/NG2$^+$ cell types, except for Per cells, expressed Olig 2. Second, although we did not do cell counts, we found no evidence that BrdU$^+$/NG2$^+$ cells colabel with astrocyte or microglial markers, a finding that agrees with other reports (Komitova et al., 2006; Kang et al., 2010; Simon et al., 2011). Third, we estimated that about 34% of all NG2$^-$/BrdU$^+$ cells were satellite cells on the cell bodies of NeuN$^+$ and Cr$^+$ neurons, about the same percentage of satellite cells that Koketsu et al. (2003) reported in a young adult *M. fascicularis* (37.4%) and a juvenile *M. fuscata* (35.7%). As noted in the Results, some satellite cells are interneurons. Astrocytes and microglial satellite cells are also known to occur but most satellite cells in the CNS are a type of oligodendrocyte (Rakic, 1985; Peters et al., 1991; Takasaki et al., 2010). Because oligodendrocytes lose NG2$^+$ antigenicity with the development of myelin proteins (Levine et al., 2001; Takasaki et al., 2010), it is likely that some BrdU$^+$/NG2$^-$ satellite cells that we found are mature oligodendrocytes.

The analysis of NG2$^+$ cell type percentages in short survival monkeys also suggested a developmental trend from simple to multibranched NG2$^+$ forms that has been shown to precede the maturation of premyelinating oligodendrocytes (Trapp et al., 1997).

There were high percentages of unbranched or simple-branched cells (Per-Elu and NG2$^+$ unknown cells) and low percentages of multibranched cells (Pld, Pldv) at 2 days and 2 weeks after BrdU administration that changed to low percentages of unbranched cells and high percentages of multibranched cells at 6 weeks post-BrdU. The average percentage NG2$^+$ multibranched cells from two, 6-week monkeys (55%; Table 3B) was just outside the upper estimate of multibranched cells in exercise monkeys that survived 15 and 27 weeks after initial BrdU injections (Table 4A). A similar developmental trend was seen in the appearance of closely paired BrdU$^+$ cells. Close pairing of BrdU$^+$ cells is a probable indicator of cell origins within the neocortex as apposed to migration from subventricular sources (Dayer et al., 2005). Our data suggests a decrease in BrdU$^+$/NG2$^+$ cell proliferation from highest percentages of cell pairs at 2 days (36%) and 2 weeks (15%) after single BrdU injections to lower percentages of cell pairs (11% and 6%) at 6 weeks after BrdU administration. The BrdU$^+$/NG2$^+$ cell percentages for 6-week monkeys largely overlapped the range of percentages from the monkeys with longer survivals after BrdU injections (2.5–10%). The 6-week period after an initial population of NG2$^+$ cells was labeled might indicate the beginning of a second cycle for these cells in the monkey motor cortex. It is known that, in mice, NG2$^+$ cells have long cell cycles (Simon et al., 2011; Hughes et al., 2013) and that proliferation of these cells decreases by two-thirds after the first division (Hughes et al., 2013). The cell cycle length in mice was calculated at 37 days in one study (Simon et al., 2011) and averaged at 18 days (range 5–40 days) in another (Hughes et al., 2013). However, a longer cell cycle for NG2$^+$ cells in monkeys might be expected based on our earlier findings that maturation times for granule cells in the monkey hippocampus were as much as 6 times longer than maturation times for these cells in rodents (Kohler et al., 2011).

Overall, the mean percentages of $BrdU^+/NG2^+$ cells from both short and long post-BrdU survival groups is about 86% of total $BrdU^+$ cells. This percentage is higher than the estimated 74% of adult born cells that are $NG2^+$ in the rat cerebral cortex (Dawson et al., 2003) and 80% in the mouse neocortex (Simon et al., 2011). Because some $NG2^+$ cells lose their antigenicity as they mature and others die off, the constancy of $NG2^+$ cells in the adult born cell population over the timepoints that we studied indicates that these cells continue to proliferate in proportion to the depletion of their numbers by cell death and maturation. The appearance of $NG2^+$ cell pairs in monkeys that survived 27 weeks after BrdU injections is evidence of their continued proliferation. Cell fate studies have shown that $NG2^+$ cells are generated continuously in the cerebral cortex of adult mice (Kang et al., 2010; Simon et al., 2011) throughout time periods as long as 70 days (Simon et al., 2011).

Some comparisons to $NG2^+$ studies in rodents

The perivascular locations and different morphologies of NG2 cells that we see in the monkey contrast with the commonly held idea, based largely on studies in mice, that 95% of NG2 cells are polydendrocytes (Nishiyama et al., 2009). In our study, the estimated total of all polydendrocytes (all multibranched $NG2^+$ cells in Table 3A) was 51%, of which 23% were polydendritic perivascular cells. It has also been reported that "a vast majority" of new cells in the visual cortex and about 74.2% of new cells in the amygdala of adult mice coexpressed NG2 and astroglial marker s-100β (Ehninger 2011). We found no colabeling of $NG2^+$ cells with either astroglia marker s-100β or GFAP or with microglia marker Iba-1.

NG2 is also expressed in mesenchymal cells, including macrophages that are excluded from the brain in normal circumstances and so were not studied herein, and vascular mural cells that include smooth muscle cells and pericytes. Both cell types have processes confined to vessel walls but pericytes lie closest to the endothelial cells, are separated from them and other cells by a basement membrane (Krueger and Bechmann, 2010; Dore-Duffy and Cleary, 2011), and label specifically with PDGFrβ antibody in mice (Winkler et al., 2010). We used these criteria (except for ultrastructural identification of the basement membrane) to estimate $NG2^+$ pericytes at 2.5% of $NG2^+$ cells. In transgenic mice, an estimated 1.5% of $NG2^+$ glial progenitor cells were pericytes (Kang et al., 2010).

Elu cells made up about a quarter of the $NG2^+$ perivascular cells. These cells, which displayed prominent nuclei and cell bodies and few cell processes that they extended into the brain parenchyma, have not been described in mice, although pericytes with processes were seen in the developing rat optic nerve (Quimby and Fern, 2011) and cells with radial processes have been identified as pericytes by other criteria (fig. 2b, Hughes et al., 2013).

There are several possible reasons why the perivascular NG2 cell types that we identified have not been described previously in rodents. First, most studies have concentrated on the polydendritic NG2 progenitor cells that differentiate into oligodendrocytes (Komitova et al., 2009; Kang et al., 2010) and deliberately excluded perivascular NG2 cells from consideration (Komitova et al., 2009; Simon et al., 2011). Also, most studies have imaged these cells at relatively low confocal magnifications as compared to the images presented in the present report and, as seen in Figure 3D–F, vessels associated with polydendritic cells were often obscured by the cell branches from these cells, particularly in images generated from confocal projection stacks. Furthermore, vessels in the parenchyma might not be seen unless specific methods are used to detect them (Fig. 2E). Finally, NG2 progenitor cells in mice are relatively smaller than in monkeys and the cytoskeletal features that we describe may be less obvious in smaller cells.

Immature calretinin interneurons

We found a consistent proportion (~7.5%) of new Cr^+ cells (but not calbindin cells) in new cell counts from tissue prepared in two separate IHC batches. $BrdU^+/GABA^+$ cells were also found but not counted. The discovery of these cells was surprising because we found no evidence of DCx labeling for immature neurons in the motor cortex and Koketsu et al. (2006) found only 2/30,000 DCx^+ neocortical cells in their study. The actual number of new Cr^+ cells/monkey was quite small. In a new cell frequency count of 24 long survival monkeys (100 cells/monkey/3 sections), four monkeys had no new Cr^+ cells and nine had 1–3 new Cr^+ cells. Furthermore, in contrast to robust labeling and well-stained processes in established $BrdU^-/Cr^+$ cells, most $BrdU^+/Cr^+$ cells were weakly labeled cell soma and only about 25% of new Cr^+ cells had bipolar or simply branched multipolar processes resembling mature calretinin interneurons.

Expression of Cr developed late but appeared to increase over time. The highest percentage of $BrdU^+/Cr^+$ cells were found in monkeys that survived 27 weeks after the first of 10 weekly injections of BrdU. We considered that new Cr^+ cells in the motor cortex might have a prolonged maturation comparable to the

hippocampal granule cells that we described in these same experimental monkeys (Kohler et al., 2011). However, we rejected this idea because even though granule cell maturation was prolonged, about 40% of granule cells were $NeuN^+$ by the end of 27 weeks. Therefore, we conclude that it is unlikely that $BrdU^+/Cr^+$ cells that we find in the motor cortex reach maturity and become functionally connected. This conclusion is in agreement with earlier ones (Rakic, 1985; Kornack and Rakic, 2001; Koketsu et al., 2003), and with the observation, based on ^{14}C birth dating of neocortical neurons in humans, that neuron birthdates in all cerebral lobes matched the age of the individual and no neurons of younger ages were detected (Bhardwaj et al., 2006).

It is possible that new, immature Cr^+ cells might have short-lived, trophic functions in the adult motor cortex. This might occur nonsynaptically, as in the secretion of reelin protein into perineuronal nets by a small percentage of calretinin interneurons (Pesold et al., 1999) or synaptically, because GABAergic neurons form functional synapses before reaching maturity (Verhage et al., 2000; Le Magueresse and Monyer, 2013). Excitatory GABAergic synapses on gray matter $NG2^+$ cells increase BDNF production in $NG2^+$ cells (Tanaka et al., 2009) and increase motility of NG2 cell processes (Haberlandt et al., 2011). Although we were unable to show evidence for synaptic contact between $NG2^+$ cells and immature $BrdU^+/Cr^+$ cells, we did find close apposition between mature Cr^+ and new $NG2^+$ cells (Fig. 6F) that supports the idea of synaptic communication between these cell types.

Technical considerations

We used data from two studies that were different with respect to the amount and frequency of BrdU injections, the species types, and the experimental conditions. However, the mean percentages of all new $NG2^+$ cells were nearly the same and the proportions of cell phenotypes were also similar for both datasets. Therefore, we concluded that differences in experimental methods did not significantly impact the data analysis. We reached the same conclusion in a separate study of granule cell maturation in the hippocampus using these same monkeys (Kohler et al., 2011).

There was considerable variability between individual animals in the same animal groupings in some $BrdU^+/NG2^+$ and $BrdU^+/Cr^+$ cell counts. Variability in counts of cells labeled with $BrdU^+$ and colabels was reported previously (Dayer et al., 2005). In part, variability in BrdU labeling might be the result of the method itself. It is known that BrdU effects the migration, cell numbers, and possibly cell survival (Breunig et al., 2007; Duque and Rakic, 2011). Furthermore, $NG2^+$ cells, the largest group of adult born cells, might have been more susceptible to negative effects of BrdU due to long maturation times for these cells. However, as noted, we found similar proportions of $BrdU^+$ labeled cells in the two study groups of monkeys even though cells labeled in monkeys with multiple-injections and longer, post-BrdU survivals were most likely to be vulnerable to the negative effects of BrdU exposure.

We found the expression of PDGFrβ in all $NG2^+$cells rather than being limited to pericytes, as Winkler et al. (2010) reported. However, because we find the same localization of PDGFrβ in pericytes along the vessel lumen, as seen in pericytes of adult mice (Winkler et al., 2010) and human embryonic tissue (Virgintino et al., 2007), we conclude that expression of PDGFrβ in other, non-pericyte $NG2^+$ cells is meaningful and that PDGFrβ expression in monkeys is different than it is in mice. We emphasize that, although PDGFrβ antibody labeling aids in the recognition of $NG2^+$ perivascular cells, classification of these cell types does not depend on use of this antibody.

Effect of exercise on NG2 cells

We anticipated that exercise might generate an increase in the proportion of new $NG2^+$ perivascular cells because exercise increased vascular volume fraction in the neostriatum (Kohler et al., 2007) and in the motor cortex (Rhyu et al., 2010) of older runner monkeys from the same experimental monkeys used in the present study. However, we did not see proportional increases in either $BrdU^+/NG2^+$ (pericytes, Elu, and Pldv cells) or in $BrdU^+/NG2^-$ perivascular cells (including endothelial cells) in any exercise group. We reasoned that this might be because new, vessel-forming cells were generated during the study's 9-week, exercise training period prior to BrdU injections, and that after a peak of new vessel-forming cell production, the relative proportions of these new cell phenotypes in exercise monkeys became comparable to new cell phenotypes in sedentary controls and short-survival monkeys. Furthermore, the exercise monkeys in our study rested 5 weeks and 12 weeks before histology, whereas an effect of exercise on $NG2^+$ cells in mice was detected immediately after exercise cessation (Simon et al., 2011). A stereological cell density study of new cell phenotypes might have detected differences due to exercise but such an analysis was not technically feasible because tissue pretreatment for BrdU immunohistochemistry disrupts generalized stains for all cell nuclei.

A percentage decrease in the Pldv cell type and percentage increases in $BrdU^+/NG2^+$ unknown cells (not

perivascular / not multibranched) and non-perivascular $BrdU^+/NG2^-$ cells were seen in the run-stop monkey group compared to control and runner groups, respectively. The decrease in percentages of Pldv cells might have resulted from cell death, loss of NG2 expression as these cells matured, or both, but the significant increase in the proportion of new, unidentified $NG2^-$ and $NG2^+$ cells in run-stop monkeys is consistent with the idea that Pldv cells mature and differentiate into another form. In mice, for example, percentages of $NG2^+$ cells were dramatically lower and percentages of mature oligodendrocytes were higher in exercised versus nonexercised subjects (Simon et al., 2011). In our study, the postexercise period changes might be related to vascular remodeling that occurred after exercise (Kohler et al., 2007; Rhyu et al., 2010). It should be noted that because run-stop monkeys survived the longest period after initial BrdU injections, the length of post-BrdU survival is another factor that might have influenced the proportions of cell phenotypes in run-stop monkey groups.

An interaction of monkey age with exercise was also suggested by the results of our experiment. Older runners had higher percentages of Per-Elu cells and lower percentages of multibranched forms compared to their counterparts, and older run-stop monkeys had higher percentages of combined perivascular phenotypes than younger run-stop monkeys. These differences might indicate a relatively slower maturation in older monkeys from simple, perivascular $NG2^+$ cells to more complex polydendritic cells in the brain parenchyma.

In the present study, we have shown that approximately half of newly generated $NG2^+$ cells in the adult monkey motor cortex are two cell types, Elu and Pldv cells, that share anatomical and immunohistochemical features with $NG2^+$ pericytes and might share functional properties as well. The proportions of both cells types, but Pldv cells in particular, were responsive to variables of the exercise experiment, although a direct relationship to exercise could not be demonstrated.

ACKNOWLEDGMENTS

The authors thank Dr. William Stallcup of the Sanford-Burnham Medical Research Institute for advice on NG2 antibody usage and Dr. Ralph Reisfeld of the Scripps Research Institute for supplying the NG2 antibody 9.2.27. We thank Dianwen Zhang, Imaging Technology Group, Beckman Institute, Sivaguru Mayandi, Core Facilities, Institute for Genomic Biology of the University of Illinois, Urbana, for assistance with confocal microscopes and Dan Sewell of the Department of Statistics, University of Illinois. We also thank Emily Underwood, Andrew Kleczek, Jessica Gu, Don Wei, Michael Chan, Amogh Belagodu, and Janet Sinn-Hanlon for technical help at various stages of the study. We thank Dr. W.K. Dong for helpful comments.

CONFLICT OF INTEREST

The authors declare no conflict of interest.

AUTHOR CONTRIBUTIONS

All authors had full access to all the data in the study and take responsibility for the integrity of the data and the accuracy of the data analysis. Study concept, design and funding: JLC, WTG; acquisition of data: JB, SJK, GBS; analysis and interpretation of data: GBS, JB, SJK; drafting of the article: GBS.

LITERATURE CITED

Barinka F, Druga R. 2010. Calretinin expression in the mammalian neocortex: a review. Physiol Res 59:665–677.

Bell RD, Winkler EA, Sagare AP, Singh I, LaRue B, Deane R, Zlokovic BV. 2010. Pericytes control key neurovascular functions and neuronal phenotype in the adult brain and during brain aging. Neuron 68:409–427.

Bhardwaj RD, Curtis MA, Spalding KL, Buchholz BA, Fink D, Bjork-Eriksson T, Nordborg C, Gage FH, Druid H, Eriksson PS, Frisen J. 2006. Neocortical neurogenesis in humans is restricted to development. Proc Natl Acad Sci U S A 103:12564–12568.

Breunig JJ, Arellano JI, Macklis JD, Rakic P. 2007. Everything that glitters isn't gold: a critical review of postnatal neural precursor analyses. Cell Stem Cell 1:612–627.

Bumol TF, Walker LE, Reisfeld RA. 1984. Biosynthetic studies of proteoglycans in human melanoma cells with a monoclonal antibody to a core glycoprotein of chondroitin sulfate proteoglycans. J Biol Chem 259:12733–12741.

Cassiani-Ingoni R, Coksaygan T, Xue H, Reichert-Scrivner SA, Wiendl H, Rao MS, Magnus T. 2006. Cytoplasmic translocation of Olig2 in adult glial progenitors marks the generation of reactive astrocytes following autoimmune inflammation. Exp Neurol 201:349–358.

Chagin VO, Stear JH, Cardoso MC. 2010. Organization of DNA replication. Cold Spring Harbor Perspect Biol 2:a000737.

Dawson MR, Polito A, Levine JM, Reynolds R. 2003. NG2-expressing glial progenitor cells: an abundant and widespread population of cycling cells in the adult rat CNS. Mol Cell Neurosci 24:476–488.

Dayer AG, Cleaver KM, Abouantoun T, Cameron HA. 2005. New GABAergic interneurons in the adult neocortex and striatum are generated from different precursors. J Cell Biol 168:415–427.

Diaz-Flores L, Gutierrez R, Madrid JF, Varela H, Valladares F, Acosta E, Martin-Vasallo P, Diaz-Flores L Jr. 2009. Pericytes. Morphofunction, interactions and pathology in a quiescent and activated mesenchymal cell niche. Histol Histopathol 24:909–969.

Dimou L, Simon C, Kirchhoff F, Takebayashi H, Gotz M. 2008. Progeny of Olig2-expressing progenitors in the gray and white matter of the adult mouse cerebral cortex. J Neurosci 28:10434–10442.

Ding YH, Li J, Zhou Y, Rafols JA, Clark JC, Ding Y. 2006. Cerebral angiogenesis and expression of angiogenic factors in aging rats after exercise. Curr Neurovasc Res 3:15–23.

Dore-Duffy P, Cleary K. 2011. Morphology and properties of pericytes. Methods Mol Biol 686:49–68.

Dore-Duffy P, LaManna JC. 2007. Physiologic angiodynamics in the brain. Antioxid Redox Signal 9:1363–1371.

Duque A, Rakic P. 2011. Different effects of bromodeoxyuridine and [3H]thymidine incorporation into DNA on cell proliferation, position, and fate. J Neurosci 31:15205–15217.

Ehninger D, Kempermann G. 2003. Regional effects of wheel running and environmental enrichment on cell genesis and microglia proliferation in the adult murine neocortex. Cereb Cortex 13:845–851.

Fang X, Burg MA, Barritt D, Dahlin-Huppe K, Nishiyama A, Stallcup WB. 1999. Cytoskeletal reorganization induced by engagement of the NG2 proteoglycan leads to cell spreading and migration. Mol Biol Cell 10:3373–3387.

Gabbott PL, Bacon SJ. 1996. Local circuit neurons in the medial prefrontal cortex (areas 24a,b,c, 25 and 32) in the monkey: I. Cell morphology and morphometrics. J Comp Neurol 364:567–608.

Goritz C, Dias DO, Tomilin N, Barbacid M, Shupliakov O, Frisen J. 2011. A pericyte origin of spinal cord scar tissue. Science 333:238–242.

Haberlandt C, Derouiche A, Wyczynski A, Haseleu J, Pohle J, Karram K, Trotter J, Seifert G, Frotscher M, Steinhauser C, Jabs R. 2011. Gray matter NG2 cells display multiple Ca2+-signaling pathways and highly motile processes. PLoS One 6:e17575.

Helfer JL, Calizo LH, Dong WK, Goodlett CR, Greenough WT, Klintsova AY. 2009. Binge-like postnatal alcohol exposure triggers cortical gliogenesis in adolescent rats. J Comp Neurol 514:259–271.

Herholz K, Buskies W, Rist M, Pawlik G, Hollmann W, Heiss WD. 1987. Regional cerebral blood flow in man at rest and during exercise. J Neurol 234:9–13.

Holmes MM, Galea LA, Mistlberger RE, Kempermann G. 2004. Adult hippocampal neurogenesis and voluntary running activity: circadian and dose-dependent effects. J Neurosci Res 76:216–222.

Hughes EG, Kang SH, Fukaya M, Bergles DE. 2013. Oligodendrocyte progenitors balance growth with self-repulsion to achieve homeostasis in the adult brain. Nat Neurosci 16: 668–676.

Isaacs KR, Anderson BJ, Alcantara AA, Black JE, Greenough WT. 1992. Exercise and the brain: angiogenesis in the adult rat cerebellum after vigorous physical activity and motor skill learning. J Cereb Blood Flow Metab 12:110–119.

Kang SH, Fukaya M, Yang JK, Rothstein JD, Bergles DE. 2010. NG2+ CNS glial progenitors remain committed to the oligodendrocyte lineage in postnatal life and following neurodegeneration. Neuron 68:668–681.

Klintsova AY, Dickson E, Yoshida R, Greenough WT. 2004. Altered expression of BDNF and its high-affinity receptor TrkB in response to complex motor learning and moderate exercise. Brain Res 1028:92–104.

Kohler S, Jennings V, Todd S, Rhyu I, Williams N, Cameron J, Greenough W. 2007. Exercise increases capillary volume in the neostriatum of macaque monkeys. Abstr Soc Neurosci 589.

Kohler SJ, Williams NI, Stanton GB, Cameron JL, Greenough WT. 2011. Maturation time of new granule cells in the dentate gyrus of adult macaque monkeys exceeds six months. Proc Natl Acad Sci U S A 108:10326–10331.

Koketsu D, Mikami A, Miyamoto Y, Hisatsune T. 2003. Nonrenewal of neurons in the cerebral neocortex of adult macaque monkeys. J Neurosci 23:937–942.

Koketsu D, Furuichi Y, Maeda M, Matsuoka N, Miyamoto Y, Hisatsune T. 2006. Increased number of new neurons in the olfactory bulb and hippocampus of adult non-human primates after focal ischemia. Exp Neurol 199:92–102.

Komitova M, Perfilieva E, Mattsson B, Eriksson PS, Johansson BB. 2006. Enriched environment after focal cortical ischemia enhances the generation of astroglia and NG2 positive polydendrocytes in adult rat neocortex. Exp Neurol 199:113–121.

Komitova M, Zhu X, Serwanski DR, Nishiyama A. 2009. NG2 cells are distinct from neurogenic cells in the postnatal mouse subventricular zone. J Comp Neurol 512:702–716.

Kornack DR, Rakic P. 2001. Cell proliferation without neurogenesis in adult primate neocortex. Science 294:2127–2130.

Krueger M, Bechmann I. 2010. CNS pericytes: concepts, misconceptions, and a way out. Glia 58:1–10.

Le Magueresse C, Monyer H. 2013. GABAergic interneurons shape the functional maturation of the cortex. Neuron 77:388–405.

Leak RK, Garbett KA, Dettmer AM, Zhang Z, Mirnics K, Cameron JL. 2012. Physical activity is linked to ceruloplasmin in the striatum of intact but not MPTP-treated primates. Cell Tissue Res 350:401–407.

Levine JM, Reynolds R, Fawcett JW. 2001. The oligodendrocyte precursor cell in health and disease. Trends Neurosci 24:39–47.

Ligon KL, Fancy SP, Franklin RJ, Rowitch DH. 2006. Olig gene function in CNS development and disease. Glia 54:1–10.

Martin R, Bowden D. 2000. Prirmate brain maps: structure of the macaque brain. Amsterdam: Elsevier.

Mouton P. 2002. Principles and practices of unbiased stereology: an introduction for bioscientists. Baltimore, MD: Johns Hopkins University Press.

Nishiyama A, Komitova M, Suzuki R, Zhu X. 2009. Polydendrocytes (NG2 cells): multifunctional cells with lineage plasticity. Nat Rev Neurosci 10:9–22.

Olah M, Ping G, De Haas AH, Brouwer N, Meerlo P, Van Der Zee EA, Biber K, Boddeke HW. 2009. Enhanced hippocampal neurogenesis in the absence of microglia T cell interaction and microglia activation in the murine running wheel model. Glia 57:1046–1061.

Ozerdem U, Grako KA, Dahlin-Huppe K, Monosov E, Stallcup WB. 2001. NG2 proteoglycan is expressed exclusively by mural cells during vascular morphogenesis. Dev Dyn 222:218–227.

Palmer TD, Willhoite AR, Gage FH. 2000. Vascular niche for adult hippocampal neurogenesis. J Comp Neurol 425: 479–494.

Paul G, Ozen I, Christophersen NS, Reinbothe T, Bengzon J, Visse E, Jansson K, Dannaeus K, Henriques-Oliveira C, Roybon L, Anisimov SV, Renstrom E, Svensson M, Haegerstrand A, Brundin P. 2012. The adult human brain harbors multipotent perivascular mesenchymal stem cells. PLoS One 7:e35577.

Pesold C, Liu WS, Guidotti A, Costa E, Caruncho HJ. 1999. Cortical bitufted, horizontal, and Martinotti cells preferentially express and secrete reelin into perineuronal nets, nonsynaptically modulating gene expression. Proc Natl Acad Sci U S A 96:3217–3222.

Peters A, Palay SL, Webster HD. 1991. The fine structure of the nervous system. New York: Oxford University Press.

Pham LD, Hayakawa K, Seo JH, Nguyen MN, Som AT, Lee BJ, Guo S, Kim KW, Lo EH, Arai K. 2012. Crosstalk between oligodendrocytes and cerebral endothelium contributes to vascular remodeling after white matter injury. Glia 60: 875–881.

Porter GA, Palade GE, Milici AJ. 1990. Differential binding of the lectins Griffonia simplicifolia I and Lycopersicon esculentum to microvascular endothelium: organ-specific

localization and partial glycoprotein characterization. Eur J Cell Biol 51:85–95.

Quimby S, Fern R. 2011. Novel morphological features of developing white matter pericytes and rapid scavenging of reactive oxygen species in the neighbouring endothelia. J Anat 219:65–77.

Rakic P. 1985. Limits of neurogenesis in primates. Science 227:1054–1056.

Rhyu IJ, Bytheway JA, Kohler SJ, Lange H, Lee KJ, Boklewski J, McCormick K, Williams NI, Stanton GB, Greenough WT, Cameron JL. 2010. Effects of aerobic exercise training on cognitive function and cortical vascularity in monkeys. Neuroscience 167:1239–1248.

Rivers LE, Young KM, Rizzi M, Jamen F, Psachoulia K, Wade A, Kessaris N, Richardson WD. 2008. PDGFRA/NG2 glia generate myelinating oligodendrocytes and piriform projection neurons in adult mice. Nat Neurosci 11:1392–1401.

Simon C, Gotz M, Dimou L. 2011. Progenitors in the adult cerebral cortex: cell cycle properties and regulation by physiological stimuli and injury. Glia 59:869–881.

Stallcup WB. 2002. The NG2 proteoglycan: past insights and future prospects. J Neurocytol 31:423–435.

Swain RA, Harris AB, Wiener EC, Dutka MV, Morris HD, Theien BE, Konda S, Engberg K, Lauterbur PC, Greenough WT. 2003. Prolonged exercise induces angiogenesis and increases cerebral blood volume in primary motor cortex of the rat. Neuroscience 117: 1037–1046.

Takasaki C, Yamasaki M, Uchigashima M, Konno K, Yanagawa Y, Watanabe M. 2010. Cytochemical and cytological properties of perineuronal oligodendrocytes in the mouse cortex. Eur J Neurosci 32:1326–1336.

Tanaka Y, Tozuka Y, Takata T, Shimazu N, Matsumura N, Ohta A, Hisatsune T. 2009. Excitatory GABAergic activation of cortical dividing glial cells. Cereb Cortex 19:2181–2195.

Trapp BD, Nishiyama A, Cheng D, Macklin W. 1997. Differentiation and death of premyelinating oligodendrocytes in developing rodent brain. J Cell Biol 137:459–468.

Trost A, Schroedl F, Lange S, Rivera FJ, Tempfer H, Korntner S, Stolt CC, Wegner M, Bogner B, Kaser-Eichberger A, Krefft K, Runge C, Aigner L, Reitsamer HA. 2013. Neural crest origin of retinal and choroidal pericytes. Invest Ophthalmol Visual Sci 54:7910–7921.

Verhage M, Maia AS, Plomp JJ, Brussaard AB, Heeroma JH, Vermeer H, Toonen RF, Hammer RE, van den Berg TK, Missler M, Geuze HJ, Sudhof TC. 2000. Synaptic assembly of the brain in the absence of neurotransmitter secretion. Science 287:864–869.

Virgintino D, Girolamo F, Errede M, Capobianco C, Robertson D, Stallcup WB, Perris R, Roncali L. 2007. An intimate interplay between precocious, migrating pericytes and endothelial cells governs human fetal brain angiogenesis. Angiogenesis 10:35–45.

Voss MW, Erickson KI, Prakash RS, Chaddock L, Kim JS, Alves H, Szabo A, Phillips SM, Wojcicki TR, Mailey EL, Olson EA, Gothe N, Vieira-Potter VJ, Martin SA, Pence BD, Cook MD, Woods JA, McAuley E, Kramer AF. 2013. Neurobiological markers of exercise-related brain plasticity in older adults. Brain Behav Immun 28:90–99.

Winkler EA, Bell RD, Zlokovic BV. 2010. Pericyte-specific expression of PDGF beta receptor in mouse models with normal and deficient PDGF beta receptor signaling. Mol Neurodegener 5:32.